Biomedical Materials

Naringenin roled octacalcium phosphate reinforced with polyvinyl alcohol composite for sarcoma affected bone repair

To cite this article before publication: Qiang Lin *et al* 2024 *Biomed. Mater.* in press https://doi.org/10.1088/1748-605X/ad3534

Naringenin Roled Octacalcium Phosphate Reinforced with Polyvinyl Alcohol Composite for Sarcomas Affected Bone repair

Qiang Lin[a], Xuzheng Wang[b], Bin Jia[c], Minghua Bai[d], and Kunzheng Wang[e*]

[a] Xi'an Jiaotong University Health Science Center, Xi'an, Shannxi Province,710061, China.

[b] Department of Orthopaedics, Jingbian County Hospital, Yulin, Shannxi Province， China.

[c] Integrated Orthopedic Department of Traditional Chinese Medicine (TCM) and Western Medicine， Hong-Hui Hospital, Xi'an Jiaotong University College of Medicine, Xi'an City, Shaanxi Province, PR China,710054

[d] Department of Orthopedic, Baoji Traditional Chinese Medicine Hospital， Baoji, Shaanxi Province, China

[e] Bone Joint Centre， Second Affiliated Hospital of Xi'an Jiaotong University， Xi'an， Shannxi Province, China.

Corresponding author: Dr. Kunzheng Wang, Bone Joint Centre, Second Affiliated Hospital of Xi'an Jiaotong University, Xi'an, Shannxi Province, China. Email ID: b13991740492@sina.com

Abstract

Osteosarcoma is a rare cancer affecting disease for children and young adults; complete healing from this condition is quite difficult. Recently, new regeneration materials have been preferred, including natural compound companied implants for affected bone repair, and it is effectively used to treat osteosarcoma disease. Hence, Octa calcium phosphate (OCP) reinforced with poly (vinyl alcohol) (PVA) and oleic acid (OA) with Naringenin (NRG) composite was prepared and studied to cure the sarcoma affected bone. The physicochemical nature of the prepared OCP, PVA/OA/OCP, and PVA/OA/OCP/NRG composite were characterized by FT-IR, SEM, and XRD techniques. The *in vitro* release of the NRG from the PVA/OA/OCP/NRG composite was evaluated by UV-visible spectroscopy and the NRG release rate was observed at 98.0 % over 24 h. Biocompatibility and cell viability of the prepared OCP, PVA/OA/OCP, and PVA/OA/OCP/NRG composite are investigated in adipose-derived stem cells (ASCs) on different days. Interestingly, the PVA/OCP/OA/NRG composite shows an increase of 74.0 % to 92.0 % in cell survival, indicating that the composite is biocompatible. Similarly, the ability of NRG in the composite is to suppress cancer cells and it was determined in lung cancer (A549) cells. NRG-loaded PVA/OCP/OA/NRG shows good inhibition ability, nearly 43 % at 72 h. From the results, the prepared composite materials can inhibit cancer cells and be viable in stem cell growth. Since the materials will serve as potential regenerative materials for sarcoma-affected bone recovery.

Keywords: Composite; Naringenin; Poly (vinyl alcohol); Octa-calcium phosphate; Osteosarcoma

Introduction

Last few decades, there has been a stable demand in the market need for regenerative treatments and repairing medicine in bone tissue engineering, especially for osteosarcoma-affected bone regenerations [1]. Osteosarcoma mainly affects young people and develops in older persons with long-standing Paget's disease in the bones [2]. The treatable condition now has a 5-year overall survival rate of 70% to 80% [3]. The method of bone disease-affected treatment has shifted the attention of numerous research fields to a variety of materials that can most closely match the characteristics of native bone [4]. During the biomineralization events, osteoblastic cells expect the physicochemical changes brought on the mineral hydrolysis process with interactions between the surfaces of calcium phosphate crystals or different inorganic ions, such as calcium and phosphate ions [5-6]. Based on the hypothesis that hydroxyapatite (HA) is formed by amorphous calcium phosphate and octacalcium phosphate (OCP) from supersaturated calcium and phosphate solutions [7]. These phases have been postulated as precursor phases in the formation of bone apatite crystals. Due to its structure and ability to transform into the thermodynamically more stable phase HA and OCP are members of the calcium orthophosphates. It has been assumed as a precursor of physiological apatite crystals [8]. Comparing OCP to other calcium phosphates, it is thought that OCP has a stronger affinity for organic molecules [9]. This is because of the structure, the comparatively empty hydrated layer, and the crystallographic planes, where it is much easier to incorporate different ions and molecules [10-15].

Octacalcium phosphate with polymers such as polymers from natural polymers such as collagen [16], gelatin [17], and hyaluronic acid [18] have been fabricated for bone implant materials. Because OCP contains a significant quantity of water molecules, it cannot be sintered without the crystalline structure breaking, unlike HA or biodegradable tricalcium phosphate (TCP) bioceramic materials [16]. As a result, compounding with polymer matrices is one method for creating the necessary morphologies for bone tissue engineering.

Poly (vinyl alcohol) (PVA) polymer is a highly functional, water-soluble, biocompatible polymer [17]. The presence of secondary alcohol groups in PVA can undergo effective nanofiber post-functionalization and the fact that the secondary alcohol functionality responds with classical chemistry [18]. PVA has special biocompatibility and biodegradability properties that make it a great choice for the design of biomedical systems [19]. Here, we prepared the OCP and PVA polymer matrix carried out in the medium of fatty acid (oleic acid) with the loading of the narigenin compound. Oleic acid (OA) is a biocompatible unsaturated fatty acid that is prevalent in blood plasma and non-human sources [20]. This molecule has demonstrated its ability to modulate stem cells because it triggers the release of angiogenic mediators by mesenchymal stem cells and controls immunomodulatory activities [21]. Additionally, it enhances cell growth because of the rise in ephrin receptors, which influence cell migration and adhesion during tissue healing [22, 23].

Similarly, natural substances offer a significant means of addressing the need to repair bone deformities and fractures. Citrus fruits are a significant source of Naringenin, a member of the flavanone family linked to several pharmacological actions [24]. Naringenin is regarded as a possible therapeutic agent in treating a variety of inflammation-related disorders, including sepsis, fibrosis, atherogenesis, and cancer [25]. Naringenin therapy reduced proinflammatory cytokine levels in macrophages by preventing NF-B activation, according to *in vivo* studies [26]. Additionally, early research reported Naringenin's benefits on bone diseases such as chronic arthritis and osteoporosis [27, 28]. Through the increase of IL-4 released by helper T cells, Naringenin may stimulate osteogenic differentiation of human periodontal ligament stem cells and decrease osteoclast genesis [29].

As we discussed, some research works are developed based on polymer-reinforced HAP materials for bone regeneration studies. Compared with other calcium phosphates, the OCP exhibits good bone regenerative properties due to the biological activity of OCP crystals that promote responses from cells surrounding bone. To the best of our knowledge, none of the reports has discussed the combination of octa calcium phosphate reinforced poly (vinyl alcohol) composite materials for bone graft materials. The addition of oleic acid and a natural compound (Naringenin) will act as an enhanced novelty of the material for improving the bio-activity of the bone graft materials in the field of orthopedic bone regeneration. The fundamental goal of the current research is to cancer-affected bone repair using a bio-compatible polymeric composite with anticancer activity and osteogenic differentiation properties derived natural compound (Naringenin), the proposed composite is to avoid the side effects of the normal cells with good regeneration ability.

Materials and Methods

Materials

Calcium acetate ($Ca(CH_3COO)_2$ (MW 158.17 & Purity 99.0%), sodium dihydrogen Phosphate (NaH_2PO_4).$2H_2O$ (MW 119.98 & Purity 99.9 %), poly(vinyl) alcohol (PVA) (MW 89,000-98,000, 99.0 % hydrolyzed), oleic acid ($C_{18}H_{34}O_2$) (MW 282.46 & Purity 99.0 %), naringenin (NRG) ($C_{15}H_{12}O_5$) (MW 272.25 & Purity 98 %) is as a substrate were purchased from Sigma-Aldrich, China. All chemicals were of analytical grade and used as such. Double distilled water (DD) is used throughout the experimental reactions.

Preparation of Octa Calcium Phosphate (OCP)

Legeros (1985) proposed method was followed for the preparation of OCP [30]. Briefly, 250 ml of 0.04M of calcium acetate (($Ca(CH_3COO)_2.H2O$) was prepared, and it was slowly added by taking 60 min into the 250 ml of 0.04M sodium dihydrogen phosphate (NaH_2PO_4).$2H_2O$ solution, which was stirred in the magnetical stirrer at 400 rpm at 67.5^0 C. The precipitate was introduced to a beaker and allowed to nucleation with stirring at 600 rpm for 30 min at 25ºC using a Teflon-coated agitator composed of aluminum red and blade. The mature octacalcium phosphate precipitate was filtered, washed with double distilled water, and dried at 60^0 C.

Preparation of PVA/OA/OCP Composite

The PVA and oleic acid embedded with OCP composite preparation was carried out based on the previous literature reported by Luppi et al, 2004 [31]. At first, 100 mg of PVA was dissolved in DD water under magnetic stirring at 60ºC. In separate, 5.0 mL of oleic acid was dissolved in 5.0 mL of ethanol solution. The above solutions are mixed and stirred under magnetic stirring for mutual interaction up to 2 h. After 2 h stirring, 500 mg of OCP was added and stirred at 25ºC for 24 h and the solvents evaporated under Rota evaporator. The dried samples were collected and stored for further reaction and characterization.

Naringenin (NRG) Loaded PVA/OA/OCP composite preparation

The NRG-loaded PVA/OA/OCP composite was prepared by the simple stirring method. Briefly, 5.0 mL of OA was initially added to the 100 mg of PVA solution and vigorously stirred under magnetic stirring for mutual interaction. After 2 h of stirring, 500 mg of OCP was added, dispersed into the above PVA/OA mixture solution, and allowed to stir for 24 h at 25ºC. After the completion of 24 h of reaction time, 20 mg of NRG compound was added to the composite solution. Then the reaction mixture was stirred under a magnetic stirrer at 25ºC for 24 h. Finally, the components were filtered and dried.

Physicochemical characterizations

Fourier Transforms Infrared Spectroscopy (FT-IR) studies

A Bruker Tensor 27 series FT-IR spectrometer was used to examine the OCP, PVA/OCP/OA, and PVA/OA/OCP/NRG composites. Each sample received 16 scans in the 4000 - 400 cm^{-1} range with a resolution of 2 cm^{-1}. For the FT-IR test, pellets were formed by smashing 0.2 gm of sample powder with 1 gm of KBr and pressing them into a clear disc.

X-ray Diffraction (XRD) studies

The prepared OCP, PVA/OCP/OA, and PVA/OA/OCP/NRG composites were characterized using X-ray diffraction to determine phase composition and crystallinity. This experiment was carried out in a Bruker D8 Advance Diffractometer using a monochromatic Cu K source operating at 40 kV and 30 mA. a speeding up. An acceleration voltage of 30 Kv and a currentof 15 mA were applied. The operating range of this test was over the 2θ range of 10 to 60° in stepscan mode with a step size of 0.02° and a scan rate of 0.02°/min.

Scanning Electron Microscopy (SEM) analysis

SEM was used to analyze the morphology of the prepared OCP, PVA/OCP/OA, and PVA/OA/OCP/NRG composites, which were operated at a 10 KV extent voltage. The sample was coated by dispersing it in DD water, the materials were studied using SEM and the matching fibers without any dispersion.

Transmittance Electron Microscopy (TEM)

The High-Resolution Transmission Electron Microscopy was taken with a JEOL JEM 2100 Co., Tokyo, Japan (HR- TEM) model. The mixture was disseminated in ethanol and applied on the Cu grid for optimum magnification for TEM research. The Selected area electron diffraction (SAED) pattern was also employed to investigate the composite's crystal structure identification.

***In vitro* NRG release**

The *in vitro* releasing behavior of NRG from PVA/OA/OCP fibrous composite was carried out through a dialysis procedure in a Phosphate buffer solution medium at pH 7.4 for 24 hours. The supernatant solution of the release medium was collected at different time intervals, and the concentration of NRG in the solution was examined in a UV-visible spectrophotometer at the maximum value of 280 nm. Finally, the proportion of NRG release was estimated by applying the following formula:

Drug release (%) = AR /AC*100

AR-Absorbance of NRG released from the composite and AC is the total quantity of NRG loaded in the composite.

Bioactivity studies in simulated body fluid (SBF)

The bioactive behavior of the prepared composite was investigated with immersion in the SBF by the formation of an apatite layer on the surface of the composite material. According to Kokubo *et al.* protocol, the SBF was prepared and the composite was soaked in SBF for 1, 7, and 14 days [32]. The concentrations (mM) of all ions that are present in the SBF solution are Sodium ion (Na^+) - 142.0; Potassium ion (K^+)- 5.0; Magnesium ion (Mg^{2+})- 5.0; Calcium ion (Ca^{2+})- 1.5, Chlorine ion (Cl^-)- 2.5; Bicarbonate ion (HCO_3^-)- 4.2; Phosphate ion (HPO_4^{2-})- 1.0; Sulphate ion (SO_4^{2-})- 0.5; and pH-7.4. The solution refreshed every couple of days. After completion of definite days, the composite was removed from the SBF solution, gently washed with DD water and the composites were dried at 60º C in a hot air oven for 5 h. Then the apatite formation on the surface of the composite was investigated through the SEM analysis.

Cell viability in adipose-derived Stem Cells (ASCs)

The adipose-derived Stem Cells (ASCs) were purchased from American type culture collection (ATCC PCS-500-012) and the cells were kept under controlled conditions in Dulbecco's modified Eagle's Medium (DMEM) in a CO_2 incubator at 37°C (with a humidifier) with low glucose (1g/L). Fetal Bovine Serum (FBS-10%) and streptomycin/penicillin (1%) were added. The cells were harvested every three days with a trypsin/EDTA solution. The effect of OCP, PVA/OCP/OA, and PVA/OCP/OA/NRG composite on ASCs growth was measured using the MTT (3-(4,5-dimethylthiazol-2-yl)-2,5-diphenyl tetrazolium bromide) test. The ASCs were seeded in a 24-well plate at a density of $4X10^4$ cells/well and co-cultured with 75 μg/mL of OCP, PVA/OCP/OA, and PVA/OCP/OA/NRG composite. MTT was used to assess ASC cell viability. After 24, 48, and 72 h of incubation, the sample solutions were removed, and MTT solutions 100 L (5 mg/mL) were added to each well plate in 1mL culture medium and incubated for 4 hours at 37°C. After that, 1mL dimethyl sulfoxide (DMSO) was added, and the supernatant medium was collected separately before centrifugation. The optical density of the superincumbent solution was measured at a wavelength of 570 nm by microplate reader.

Cytotoxicity effect against Human lung cancer (A549) cells

Cell toxicity was investigated using Human lung cancer (A549) cells obtained from the American type culture collection (ATCC PCS-500-012). A549 cells were cultured for 24 h in 24-well plates containing Dulbecco's modified eagle medium (DMEM) supplemented with 10% FBS and penicillin 100 U/mL-streptomycin (100 U mL-1) (Gibco, Grand Island, CA, USA). The cells were cultured in CO_2 and monitored using MTT test procedures at 37°C. The 75 μg/mL of composite was evaluated on cells at 24, 48, and 72 h. The OD values were measured at a maximum wavelength of 490 nm. The morphology of the composites was studied using optical microscopy, and the cytotoxicity of the composites was calculated using the formula below.

$$\mathit{Cytotoxicity}\ (\%) = \frac{\text{Test sample}}{\text{Control}} \times 100$$

Statistical analysis

The numerical data were all reported as the mean standard deviation of individual values. GraphPad Prism software version for Windows (GraphPad Software Inc., La Jolla, CA, USA) was used for statistical analysis. Statistical analysis with a $^*p<0.05$ value was judged significant.

Results and Discussion

FT-IR spectroscopy analysis

FT-IR spectroscopy analysis was subjected to investigate the chemical functionality changes in the formation of OCP, PVA/OCP/OA, and PVA/OA/OCP composite, and the spectrum was given in Figure 1. Initially, the OCP was determined, and the FTIR spectrum is presented in Figure 1a. The fundamental molecular components of PO_4^{3-} in OCP were observed in the 1200-550 cm^{-1} region. The featured peaks at 560 cm^{-1}, 945 cm^{-1}, 1034 cm^{-1}, and 1288 cm^{-1} correspond to the stretching vibrations of PO_4^{3-} group presence in the OCP. The OH^- ions are recognized by observing the wide-ranging band from around 3700 cm^{-1} to 3000 cm^{-1}. The height of the peak is centered at about 3472 cm^{-1}; that's a typical mission of the stretching vibration of OH^- ions. Characteristic vibration of PVA polymer and OA combined OCP composite was determined, and the spectrum was presented in Figure 1b. The occurrence of absorption peaks at 560 cm^{-1}, 714 cm^{-1}, 945 cm^{-1}, 1034 cm^{-1}, 1122 cm^{-1}, and 1288 cm^{-1} establishes the presence of PO_4^{3-} ions of OCP within the PVA/OCP/OA composite. Characteristic peaks of PVA had been as received from the subsequent peaks inside the spectra, as a large (OH^-) absorption stretching band, determined at 3472 cm^{-1}, indicating the presence of polymeric affiliation of the unfastened hydroxyl organizations and bonded O–H stretching vibration [33]. The characteristic peaks of oleic acid were obtained in the regions of 2855 cm^{-1} and 2932 $cm^{-1,}$ and they responded to the $-CH_2$ symmetric stretch and the asymmetric stretch, respectively. Similarly, the pure oleic acid stretching frequency was reported by the previously reported chitosan and PLGA matrix system [34]. The PLGA matrix was stabilized by different concentrations of chitosan with oleic acid for drug delivery applications. The FT-IR spectra of the PVA/OCP/OA/NRG composite represent the additional functional peaks of NRG from the PVA/OCP/OA (Figure 1c). The peaks 835 cm^{-1} and 1718 cm^{-1} for -C=O stretching, 1235 cm^{-1} for -C-O stretching, and 2721 cm^{-1} are due to the C=C and C-C of the aromatic ring of the NRG compounds present in the PVA/OCP/OA/NRG composite. Shuo Wang et al. reported the NRG-loaded PLGA nanospheres for the antibacterial analysis; in this report, the NRG has observed a similar pattern of FTIR spectrum that resembles the current research report [35].

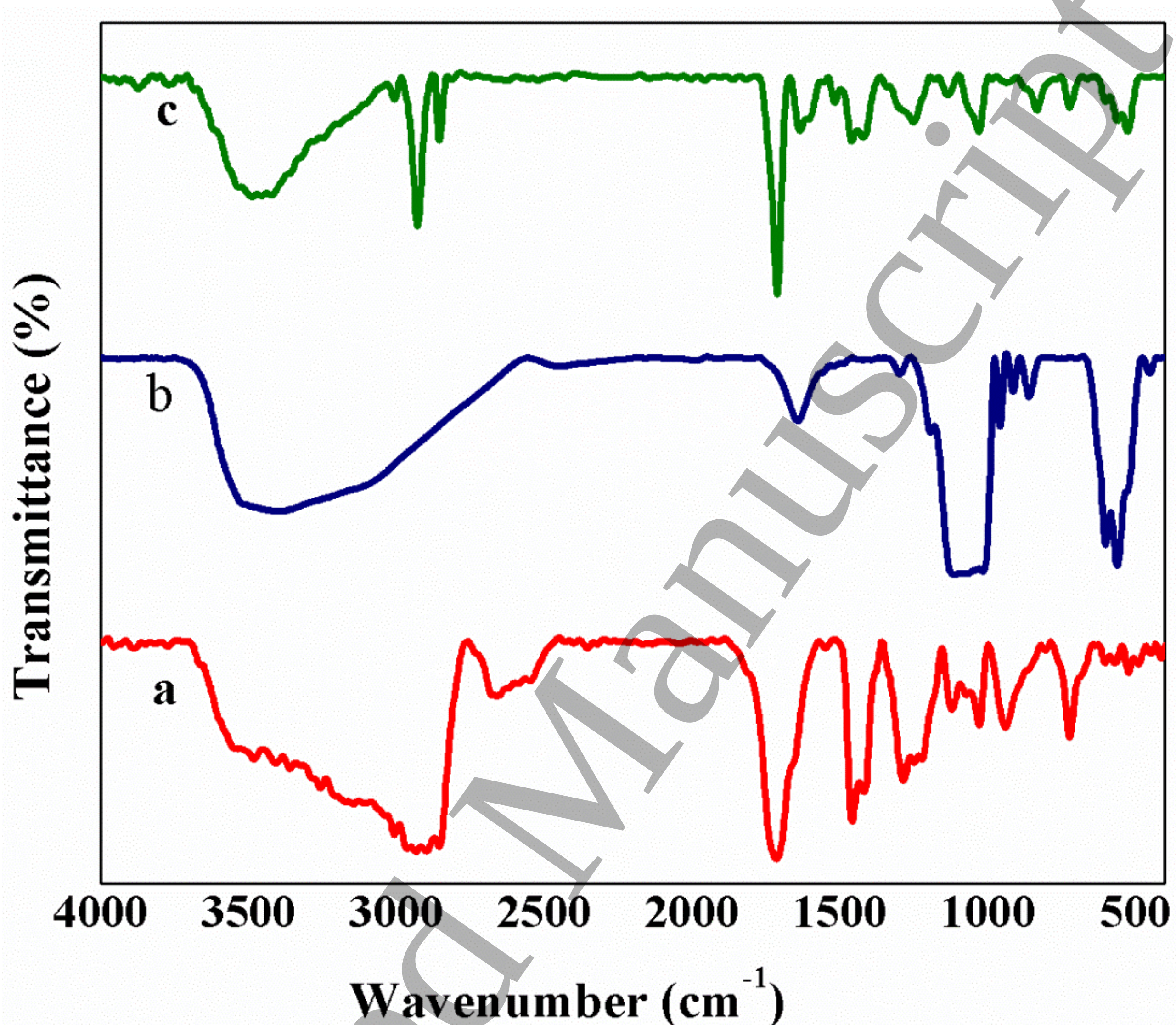

Figure 1. FT-IR spectrum of (a) OCP, (b) PVA/OCP/OA, and (c) PVA/OCP/OA/NRG composite.

XRD analysis

The XRD evaluation was used to analyze the crystalline and segment content of the inorganic part of the prepared OCP, PVA/OCP/OA, and PVA/OCP/OA/NRG composites. XRD patterns of the OCP ceramic, PVA/OCP/OA, and PVA/OCP/OA/NRG polymer ceramic fibrous composites are shown in Figure 2. The diffraction peak in Figure 2a corresponds to the OCP ceramic, which revealed that peaks at 2θ values of 17.1^0, 25.9^0, 28.9^0, and 34.1^0 were observed and could be assigned to the OCP pattern in the JCPS card # 26-1056. The characteristic pattern of OCP was confirmed for the formation such as (002), (151) and (150), (260), (070) [36]. The XRD spectrum of the PVA/OCP/OA composite is given in Figure 2b. The polymer and OCP ceramic keep their crystalline behavior inside the composite, indicating a good-sized change in their crystal structure. It also reinstates the confirmation that OCP is finely and uniformly dispersed within the matrix, similar to the real bone in which OCP is uniformly distributed within the polymeric OCP composite. The PVA molecule was at around 2θ values of 19.6º and $20.8^{0,}$ representing the addition of PVA in the OCP. Furthermore, the OA molecule in the PVA/OCP/OA revealed the new peaks at 2θ values of 11.7^{0} and 34.0.0º. Similarly, the previous report of chitosan and oleic acid film showed two major broad crystalline peaks at 7.9° and 23.1° [37], but in our case, it was observed the sharp peaks at 11.7^{0} and 34.0.0º and due to the interaction of the OA with OCP and PVA components [38]. Figure 2c corresponds to the PVA/OCP/OA composite with NRG compounds, and the crystalline peaks at 2θ values of 42.3º and 36.4º could be detected due to the NRG in the PVA/ OCP/OA/NRG composite. These diffraction peaks confirmed the formation of a PVA/OCP/OA/NRG composite with a reduced crystalline structure. The structural characteristics of OCP determine its unique *in vivo* behavior in the XRD pattern of all the formulations. OCP's two-layer structure was made up of hydrate and apatite layers that participated in ion exchange processes at the phase boundary between the material crystals and the environment. The high adsorption capacity of OCP crystals is determined by their high surface area and activity for interacting with biological molecules. It has been proposed that the number of adsorption sites changes during OCP hydrolysis to HA, which can impact new bone formation [39].

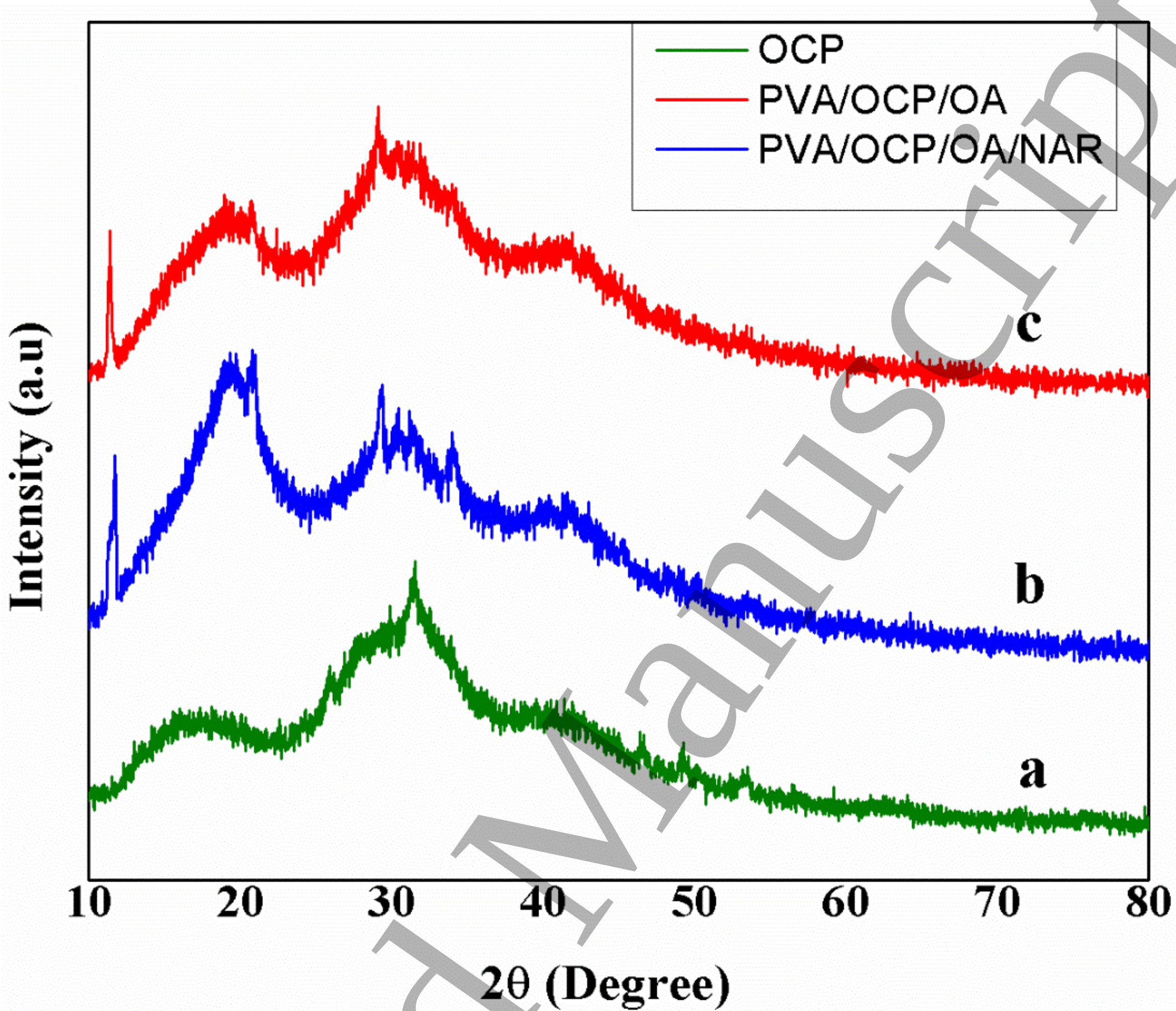

Figure 2. XRD diffraction pattern of the prepared (a) OCP, (b) PVA/OCP/OA, and (c) PVA/OCP/OA/NRG composites

Surface Morphology analysis

The surface structure of the pure OCP, PVA/OCP/OA, and PVA/OCP/OA/NRG composite was observed using SEM and TEM techniques, and the results are presented in Figures 3 and 4, respectively. The characterized result of SEM morphology of all the materials is shown in Figure 3. The SEM morphology in Figure 3a corresponds to the OCP ceramic. The OCP formed a rod-like structure with a smooth surface. The rod-like structure of the OCP is clearly observed and it correlated with the TEM observation in Figure 4a. The morphology of the PVA particle formation with the oleic acid medium was spherical, and it clearly shows the oleic acid coating on the surface of the PVA particles in Figure 3b. It can also noted in the TEM morphology in Figure 4b. The PVA/OA is noted as spherical with oily-coated morphology. After the formation of composite OCP with PVA and oleic acid, the spherical structure is maintained with some deviated morphology, and it is evidenced the OCP completely interacted with PVA and oleic acid and formed as spherical particles (Figure 3c). The rod-like structure of OCP inside the PVA/OCP is clearly observed in the TEM morphology of PVA/OCP/OA in Figure 4c. After the load of NRG in the PVA/OCP/OA, the surface morphology was observed as spherical morphology in the SEM technique (Figure 3d), and highly dense particle was observed in the TEM morphology of PVA/OCP/OA/NRG Composite (Figure 4d). It looks like an extracellular matrix with a white composite-like morphology. The native mimicking extracellular matric-derived biomaterials form a dynamic environment that can be digested, remodeled, and replaced during cell treatment [40]. The chemical nature of the materials and surface morphology both are important in the cell response of the composite materials in osteogenesis. Curious morphologies of the Inorganic materials with companied polymers and their functionalities might be capably used to further develop composite properties in the mass and along pore surface-advancing *in vitro* and *in vivo* rigid tissue in development [41].

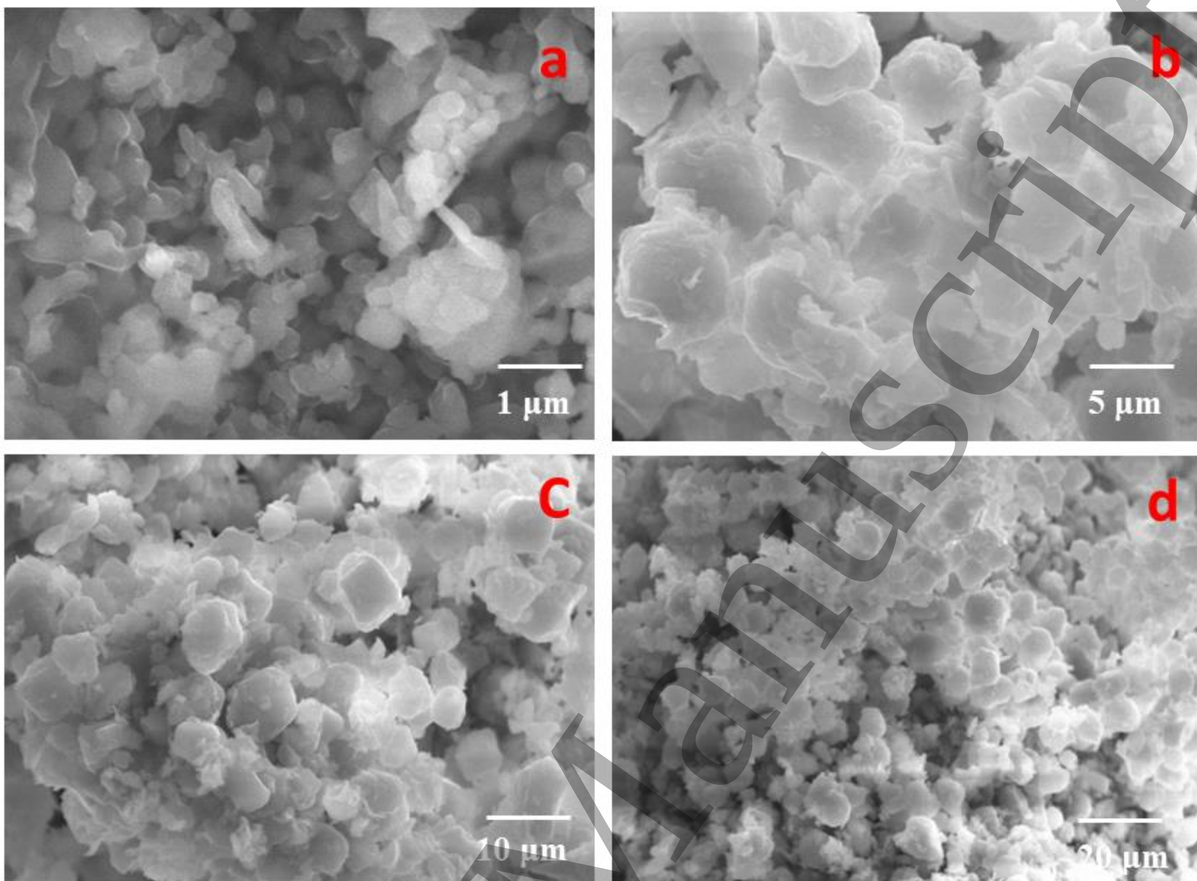

Figure 3. The SEM surface morphology of (a) OCP (1 µm), (b) PVA/OA (5 µm), (c) PVA/OCP/OA(10 µm), and (C) PVA/OCP/OA/NRG (20 µm) composites

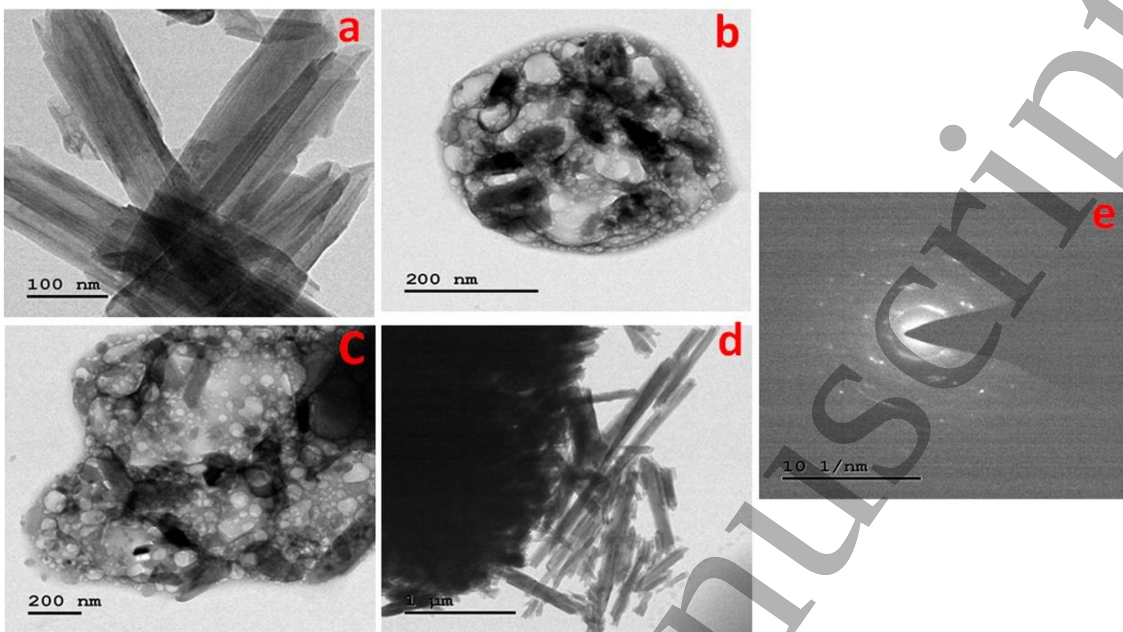

Figure 4. TEM morphology of (a) OCP (100 nm), (b) PVA/OA (200 nm), (c) PVA/OCP/OA (200 nm), (d) PVA/OCP/OA/NRG (1 μm) composite, and (e) SCAD pattern of PVA/OCP/OA/NRG composites.

***In vitro* drug release**

The main aim of the *in vitro* NRG release analysis is the self-repairing materials for sarcoma-affected bone repair through the sustainable release of the compound from the composite. The NRG-loaded PVA/OCP/OA/NRG composites are subjected to analysis of the NRG release from the composite. In this regard, the *in vitro* drug release at pH 7.4 was studied, and the NRG release rate was observed at 98.0 % over 24 h from the PVA/OCP/OA/NRG composite. It could be understood that the PVA/OCP/OA/NRG composite demonstrated the required quantity of NRG release with an initial burst release observed and followed by a constant releasing rate. It was noted that the release was continuous and could be partially due to the breakage of the bond between the NRG and PVA/OCP/OA at pH 7.4. The release rate further confirms that the composite has the potential for curing sarcoma-affected bone by the initials burst release NRG compound and serves to help the new bone formation.

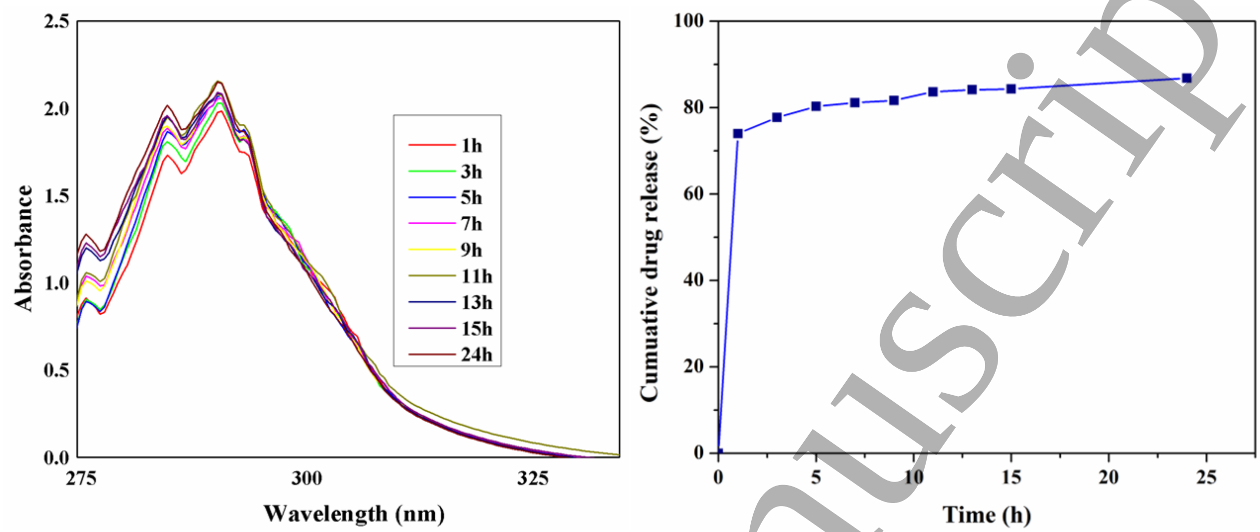

Figure 5. The drug release profile of NRG drug from PVA/OCP/OA composite. (B) Encapsulation efficiency of NRG on PVA/OCP/OA composite (C) Cumulative drug release pattern

Bioactivity analysis in the SBF solution

The hydroxyapatite formation on the surface of the prepared OCP and PVA/OCP/OA/NRG composite was observed by the SEM technique after the SBF immersion on different days, and the results are presented in Figure 6. As the day increased, the growth of HAP increased on the surface of both materials. Compared with OCP, PVA/OCP/OA/NRG composite shows the good formation of the HAP on the surface of materials. At 14 days, good HAP crystal on the surface of the materials because the OCP has good nucleation of HAP formation. Several studies have investigated the *in vivo* OCP reaction at various hydrolysis rates to the HAP formation [42, 43]. When compared to the OCP, hydrolyzed OCP to Ca-deficient HAP dramatically inhibited bone growth [42].

On the other hand, partially hydrolyzed OCP increased bone growth much more than other calcium phosphate compounds [43]. During hydrolysis, OCP structural changes alter its chemical-physical properties. The degree of solution supersaturation stipulated by the chemical composition of the solution environment controls the rate of OCP hydrolysis [44]. In this regard, depending on the treatment period and pH value, this solution generates varying degrees of OCP hydrolysis to the HAP crystal formation.

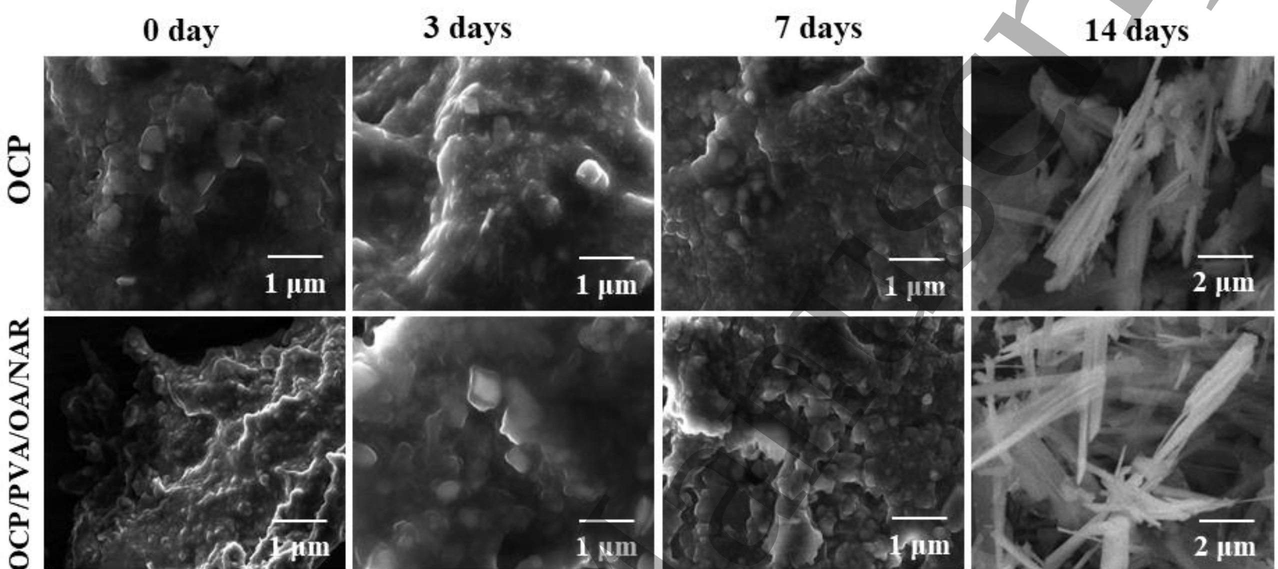

Figure 6. SEM morphology for the hydroxyapatite formation on the surface of the (a) OCP, (b) PVA/OA, (c) PVA/OCP/OA, (d) PVA/OCP/OA/NRG composite immersed in the SBF solution at 0 day, 3 days, 7 days, and 14 days.

***In vitro* cell viability of the composites**

Biocompatibility is an essential requirement for any material in the biological function or materials utilized in bone repair/regeneration analysis [45]. Biocompatibility is a substance's ability to elicit appropriate immune responses during tissue regeneration [46]. The cell viability of the materials, such as OCP, PVA/OCP/OA, and PVA/OCP/OA/NRG, was investigated in the ASCs by the MTT assay analysis. The absorbance value at 570 nm reflects the living cells quantity in the culture medium. The percentage of cell viability at 24, 48, and 72 h cultivation of 75 µg mL^{-1} of the composite is displayed in Figure 7. The OCP, PVA/OCP/OA, and PVA/OCP/OA/NRG displayed noticeable cell viability. The day increased, and the cell viability was increased compared with the control. In the PVA/OCP/OA/NRG composite cultured cells, the cell growth was increased from 74.0 % to 92.0 % compared with other composite and control. Octacalcium phosphate is the main source of bone; CaP is continuously employed to stimulate the development of new bone. However, this does not guarantee that the actual process of regeneration will be successful. The primary factor is the addition of cells, macromolecules, and blood vessels to the bone [47]. Since the PVA/OCP/OA/NRG composite shows an increase of 92 % in cell survival, indicating that the presence of NRG in the composite is bioactive with stem cell differentiation. Several recent reports of research have said that the addition of Naringenin is effective in enhancing the proliferation of osteogenic cell differentiation [48, 49]. Zhou et al. reported that osteogenic differentiation inhibits osteoclastogenic differentiation directly by Naringenin compound, and the researcher also noted Naringenin's role in improving in the equilibrium bone formation and bone resorption by altering macrophage polarisation and cytokine release in the immunological microenvironment [48]. Similarly, as reported by Zhang et al., NRG has stimulated the hPDLSC proliferation and endothelial differentiation, activating the SDF-1/CXCR4 signaling pathway [49]. In order to improve the osteogenic differentiation of hPDLSCs, the NRG activates the SDF-1 signaling pathway. Since the cell viability and differentiation of the stem cells are influenced by the presence of NRG in the PVA/OCP/OA/NRG composite, all coatings samples are biocompatible with the cells and therefore favor cell differentiation and adhesion.

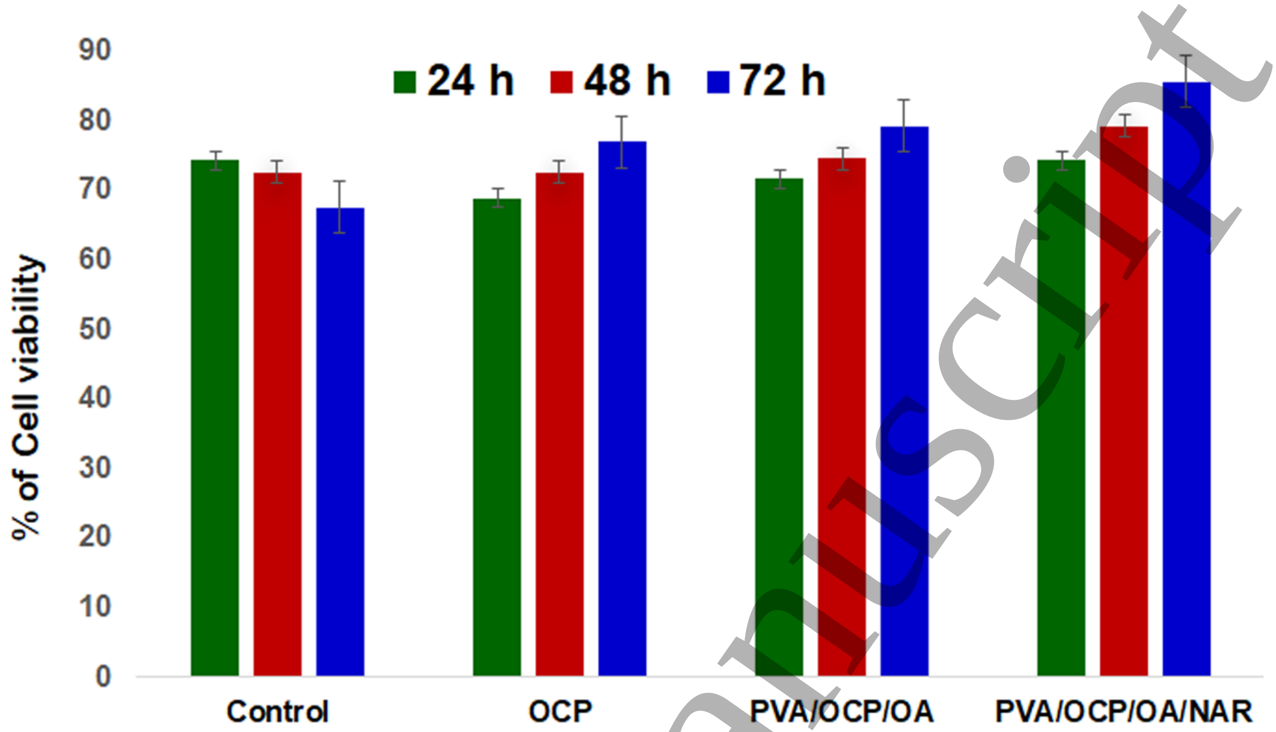

Figure 7. The cell viability of control, OCP, PVA/OA, PVA/OCP/OA, and PVA/OCP/OA/NRG composite in the adipose-derived stem cells (ASCs) at 24 h, 48 h, and 72 h.

Optical morphology of ASCs cells

Figure 8 shows the morphological changes in the cell growth, differentiation, and death by the treated OCP, PVA/OCP/OA, and PVA/OCP/OA/NRG composites. The cell morphology was obtained by a microscopic analysis after 24, 48, and 72 h incubation. The micrographs indicated that the density and growth of the cells increased with the increasing of days at 75 μg/ml concentration. In these microscopic investigations, uniformly enforced living cells tended to form larger formations, whereas dead cells were seen as ruptured cell morphology. This research also indicates that the treated composites have strong biocompatibility with stem cells and their differentiation to osteoblast-like cells for orthopedic applications at lower concentrations. The micrograph images showed that the cells were intact and stress-free without any apparent structural variations. MTT assay and cell viability indicated that prepared samples had strong biocompatibility to osteo differentiation nature. These consistent data on the beneficial benefits of octa calcium phosphate reinforcement in polyvinyl alcohol, oleic acid, and naringenin molecule, which is also evidence of the non-toxicity of OCP, PVA/OCP/OA and PVA/OCP/OA/NRG is in excellent agreement available in the literature [50-52]. These results also affirm the beneficial impact of the hybrid nanocomposite as a bone-replacement material in orthopedic implants.

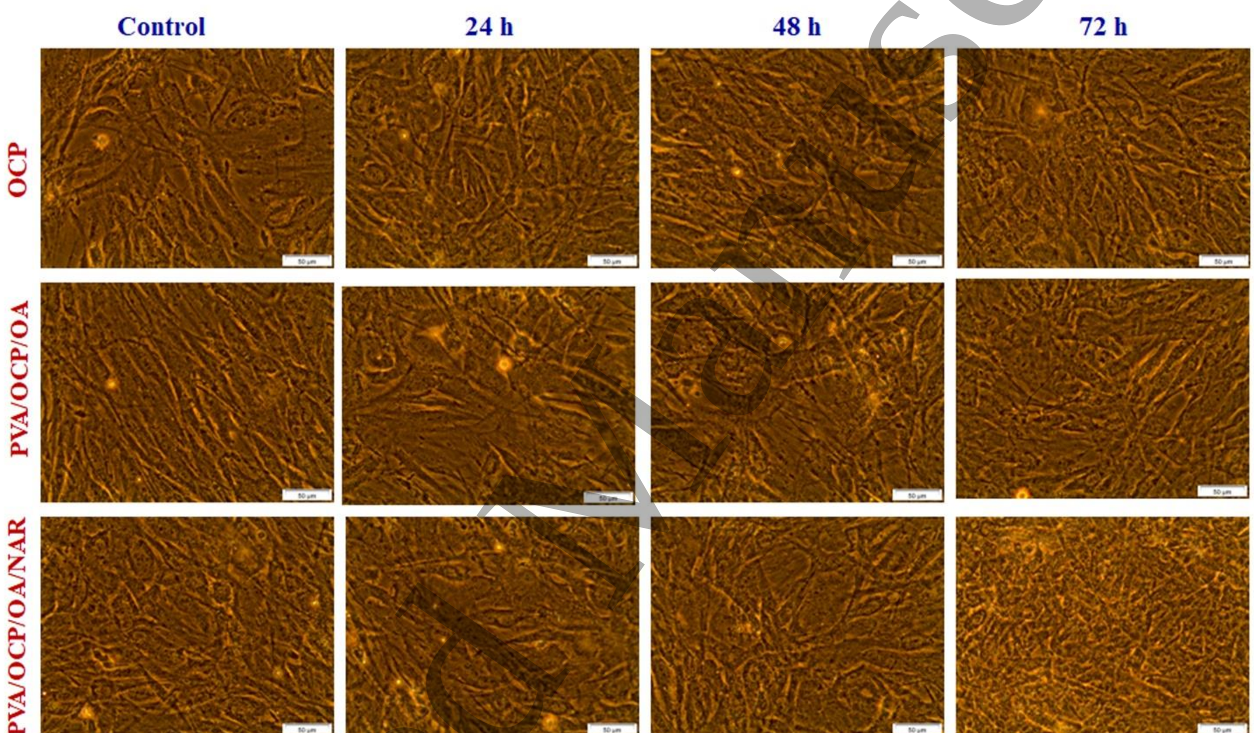

Figure 8. Optical images of cell growth treated with control, OCP, PVA/OA, PVA/OCP/OA, and PVA/OCP/OA/NRG composite at 24 h, 48 h, and 72 h.

Cytotoxicity analysis

The main aim of the cytotoxicity analysis against A549 cells is to know the anti-cancer effect of the prepared composites. Figure 9 shows the cytotoxicity percentage of OCP, PVA/OCP/OA, and PVA/OCP/OA/NRG composite against the A549 cells. The OCP, PVA/OCP/OA, and PVA/OCP/OA/NRG composite cytotoxicity against the A549 cells was investigated at 24, 48, and

72 h. With the increasing of time, the cytotoxicity was increased, and the composite OCP did not induce any toxicity against A549 cells. However, the NRG incorporated PVA/OCP/OA/NRG was observed in good cytotoxicity in the A549 cells and it observed 43 % inhibition ability in the cancer cell at 72 h. Naringenin demonstrated the ability to block IL-6's and it is the ability to regulate the expression of the genes linked to apoptosis of cancer cells. These findings showed that a Naringenin-cyclophosphamide combination could be a powerful chemotherapeutic regimen for treating breast cancer since it inhibits proliferative signaling and promotes apoptosis to a larger extent than either chemical alone [53].

The cytotoxicity effects of the OCP, PVA/OCP/OA, and PVA/OCP/OA/NRG composite against the A549 cell morphology were observed in Figure 10. With the increasing incubation days, A549 cells began to exhibit differences in the toxicity effects of OCP, PVA/OCP/OA, and PVA/OCP/OA/NRG, and it was determined that OCP, PVA, OA, and NRG had the ability inhibit the cancer cells. The previous researchers predicted OCP is a useful material for carrying bioactive molecules for bone cancer [54]. NRG has incorporated PVA/OCP/OA composite exhibits good toxicity against the cancer cells because of the composites. This result proved that the PVA/OCP/OA/NRG composites inhibited cancer cell proliferation. NRG is one of the most effective suppressions of cancer cells.

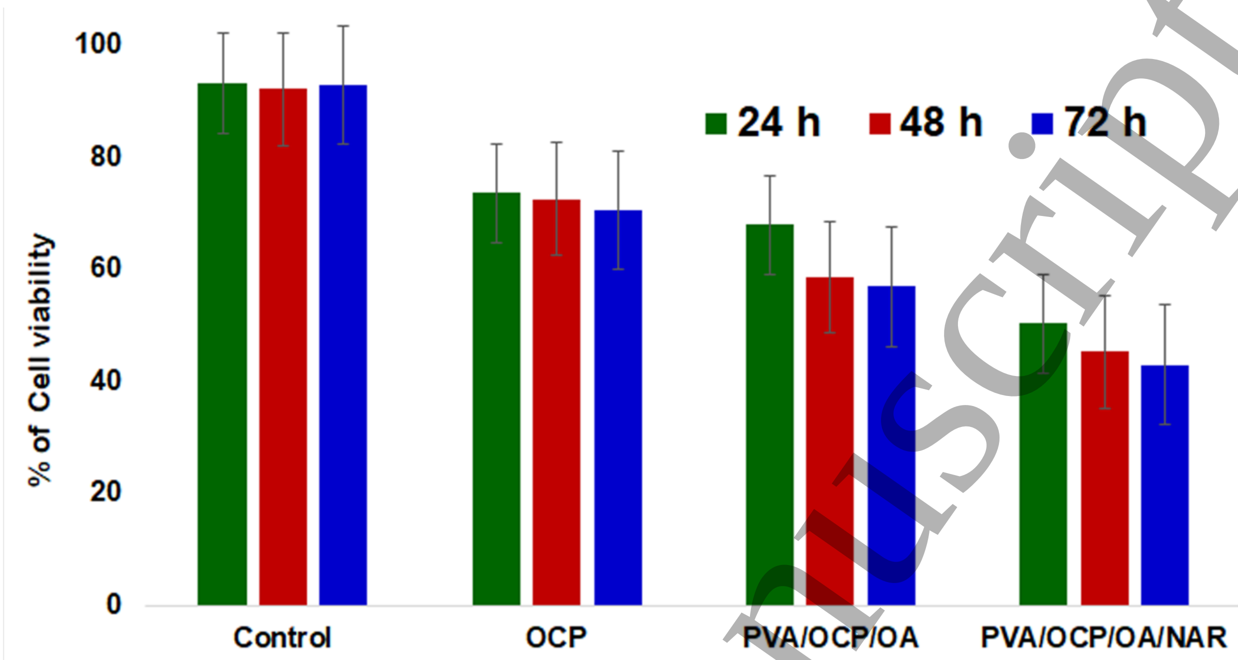

Figure 9. Cytotoxicity against human lung cancer cell (A549) by the control, OCP, PVA/OA, PVA/OCP/OA, and PVA/OCP/OA/NRG composite at 24 h, 48 h, and 72 h.

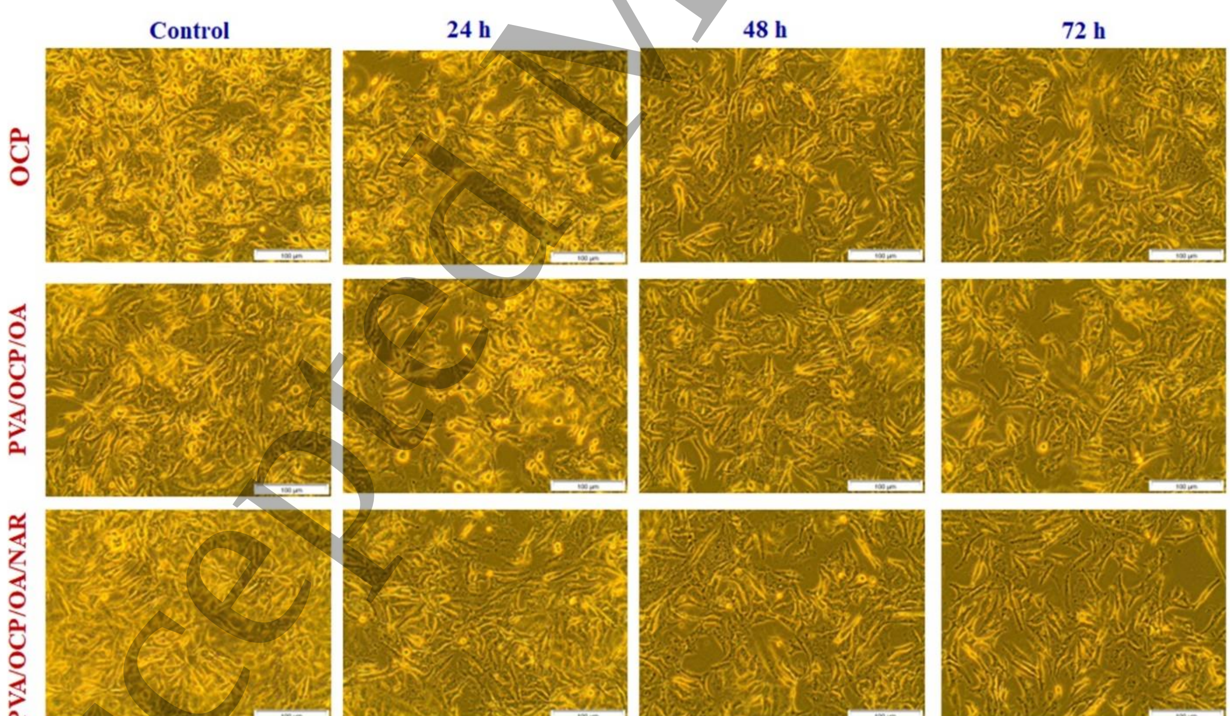

Figure 10. Optical images of cell morphology treated with OCP, PVA/OCP/OA, PVA/OCP/OA/NRG composite, and control at 24 h, 48 h, and 72 h.

Conclusion

This study described a unique composite of a bio-ceramic and biodegradable polymer as a biocompatible material. Polyvinyl alcohol (PVA) and Octa calcium phosphate (OCP) composites were used to simulate the inorganic components of bone, while Oleic acid (OA) was used to enhance osteogenesis qualities, and NRG was used as an anticancer medicine. The blending method was used to fabricate the PVA/ OCP/ OA/ NRG composite made up of these components that mimicked the bone matrix and delivery of the anticancer nature of the NRG compound. The FT-IR and XRD characterization tests confirmed that the produced material is identical to our target composite, with good purity and predicted crystallinity phases. SEM and TEM inspection validated the composite materials. Finally, the NRG was released from the composite in a regulated manner, with 98 percent of the drug released over 24 hours, as determined by dialysis. Remarkably, the PVA/OCP/OA/NRG composite shows an increase in better cell viability, and the ability of NRG in the composite is capable of suppressing cancer cells and it was determined in lung cancer (A549) cells. As a result, the PVA/OCP/OA/NRG composite will serve as a better bio-material for sarcoma disease-affected bone repair.

Declaration

Competing interests: The authors have no conflicts of interest to declare that are relevant to the content of this article.

Ethical Approval: Not applicable.

Consent for publication: Not Applicable

Availability of data and materials: All data generated or analyzed during this study are included in this published article.

Authors' contributions: Manuscript writing: Qiang Lin, Xuzheng Wang, Bin Jia, Minghua Bai; Making figures, calculations, and interpretation: Qing Guo, Zheng Li, and Fang Cao; Supervising and reviewing: Kunzheng Wang

References

1. Sumathra M, Rajan M, Praphakar R A, Marraiki N and Elgorban A M 2020 In Vivo Assessment of a Hydroxyapatite/κ-Carrageenan-Maleic Anhydride-Casein/Doxorubicin Composite-Coated Titanium Bone Implant *ACS Biomater. Sci. Eng.* **6** 1650-1662
2. Chen F M and Liu X 2016 Advancing biomaterials of human origin for tissue engineering *Prog. Polym. Sci.* **53** 86-168
3. Sumathra M and Rajan M 2019 Pulsed Electrodeposition of HAP/CPG-BSA/CUR Nanocomposite on Titanium Metal for Potential Bone Regeneration *ACS Appl. Bio Mater.* **2** 4756-4768
4. Tang S, Dong Z, Ke X, Luo J and Li J 2021 Advances in biomineralization-inspired materials for hard tissue repair *Int. J. Oral. Sci.* **13** 42
5. Hong M H, Lee J H, Jung H S, Shin H and Shin H 2022 Biomineralization of bone tissue: calcium phosphate-based inorganics in collagen fibrillar organic matrices *Biomater. Res.* **26** 42
6. Yang R, Wang R, Abbaspoor S, Rajan M, Jalil A T, Saleh M M and Wang W 2023 *In vitro* and in vivo evaluation of hydrogel-based scaffold for bone tissue engineering application *Arab. J Chem.* **16** 104799
7. Hoeher A J, Mergelsberg S T, Borkiewicz O J and Michel F M 2021 Impacts of initial Ca/P on amorphous calcium phosphate *Cryst. Growth Des.* ***21*** 3736-3745
8. Suzuki O 2013 Octacalcium phosphate (OCP)-based bone substitute materials *Jpn. Dent. Sci. Rev.* **49** 58-71

9. Yang X, Gao X, Gan Y, Gao C, Zhang X, Ting K, Wu B M and Gou Z 2010 Facile synthesis of octacalcium phosphate nanobelts: growth mechanism and surface adsorption properties *J. Phys. Chem. C* **114** 6265-6271

10. Liu Y, Cooper P R, Barralet J E and Shelton R M 2007 Influence of calcium phosphate crystal assemblies on the proliferation and osteogenic gene expression of rat bone marrow stromal cells *Biomater.* **28** 1393-1403

11. Selvakani Prabakaran, Mariappan Rajan, Osteogenic and Bacterial inhibition potential of natural and synthetic compounds loaded metal-ceramic composite coated Titanium implant for orthopedic applications, New Journal of Chemistry, 2021,**45**, 15996-16010

12. Yang Gao, Mohan Anne Seles, and Mariappan Rajan, Role of bioglass derivatives in tissue regeneration and repair: A review, Reviews on Advanced Materials Science 2023; 62: 20220318

13. Shelton R M, Liu Y, Cooper P R, Gbureck U, German M J and Barralet J E 2006 Bone marrow cell gene expression and tissue construct assembly using octacalcium phosphate microscaffolds *Biomater.* 27 2874-2881

14. Bigi A, Bracci B, Cuisinier F, Elkaim R, Fini M, Mayer I, Mihailescu I N, Socol G, Sturba L and Torricelli P 2005 Human osteoblast response to pulsed laser deposited calcium phosphate coatings *Biomater.* **26** 2381-2389

15. Kaneko H, Kamiie J, Kawakami H, Anada T, Honda Y, Shiraishi N, Kamakura S, Terasaki T, Shimauchi H and Suzuki O 2011 Proteome analysis of rat serum proteins adsorbed onto synthetic octacalcium phosphate crystals *Anal. Biochem.* **418** 276-285

16. Brown W E 1962 Octacalcium phosphate and hydroxyapatite: Crystal structure of octacalcium phosphate *Nature* **196** 1048-1050

17. Xue J, Wu T, Dai Y and Xia Y 2019 Electrospinning and Electrospun Nanofibers: Methods, Materials, and Applications *Chem. Rev.* **119** 5298-5415

18. Song Q, Prabakaran S, Duan J, Jeyaraj M, Mickymaray S, Paramasivam A and Rajan M 2021 Enhanced bone tissue regeneration via bioactive electrospun fibrous composite coated Titanium orthopedic implant *Int. J. Pharm.* **607** 120961

19. Liu C, Wu Y, Yu A and Li F 2014 Cooperative fabrication of ternary nanofibers with remarkable solvent and temperature resistance by electrospinning *RSC Adv.* **4** 31400

20. Coniglio S, Shumskaya M, 2023 Vassiliou E Unsaturated Fatty Acids and Their Immunomodulatory Properties *Biology.* 12(2) 279.

21. Tran P H L, Tran T T D and Lee B J 2013 Enhanced solubility and modified release of poorly water-soluble drugs via self-assembled gelatin-oleic acid nanoparticles *Int. J. Pharm.* **455** 235-240

22. Smith A N, Muffley L A, Bell A N, Numhom S, and Hocking A M 2012 Unsaturated fatty acids induce mesenchymal stem cells to increase secretion of angiogenic mediators *J. Cell. Physiol.* **227** 3225-3233

23. Jung Y H, Lee S J, Oh S Y, Lee H J, Ryu J M and Han H J 2015 Oleic acid enhances the motility of umbilical cord blood derived mesenchymal stem cells through EphB2-dependent F-actin formation *Biochim. Biophys. Acta* **1853** 1905-1917

24. Stabrauskiene J, Kopustinskiene D M, Lazauskas R and Bernatoniene J 2022 Naringin and Naringenin: Their Mechanisms of Action and the Potential Anticancer Activities *Biomedicines* **10** 1686

25. Zhou X, Zhang Z, Jiang W, Hu M, Meng Y, Li W, Zhou X and Wang C 2022 Naringenin is a Potential Anabolic Treatment for Bone Loss by Modulating Osteogenesis, Osteoclastogenesis, and Macrophage Polarization *Front. Pharmacol.* ***13*** 872188

26. Yang J, Liu L, Li M, Huang X, Yang H and Li K 2021 Naringenin inhibits pro-inflammatory cytokine production in macrophages through inducing MT1G to suppress the activation of NF-κB *Mol. Immunol.* **137** 155-162

27. Kaczmarczyk-Sedlak I, Wojnar W, Zych M, Ozimina-Kamińska E and Bońka A 2016 Effect of dietary flavonoid Naringenin on bones in rats with ovariectomy-induced osteoporosis *Acta Pol. Pharm.* ***73*** 1073-1081

28. Manchope M F, Artero N A, Fattori V, Mizokami S S, Pitol D L, Issa J P M, Fukada S Y, Cunha T M, Alves-Filho J C, Cunha F Q, Casagrande R and Verri Jr W A 2018 Naringenin Mitigates Titanium Dioxide (TiO_2)-Induced Chronic Arthritis in Mice: Role of Oxidative Stress, Cytokines, and NFκB *Inflamm. Res.* **67** 997-1012

29. Nor Muhamad M L, Ekeuku S O, Wong S K and Chin K Y 2022 A Scoping Review of the Skeletal Effects of Naringenin *Nutrients* **14** 4851

30. LeGeros R Z 1985 Preparation of octacalcium phosphate (OCP): a direct fast method *Calcif. Tissue Int.* **37** 194-197

31. Luppi B, Bigucci F, Cerchiara T, Andrisano V, Pucci V, Mandrioli R and Zecchi V 2005 Micelles Based on Polyvinyl Alcohol Substituted with Oleic Acid for Targeting of Lipophilic Drugs *Drug Deliv.* **12** 21-26

32. Kokubo T, Takadama H, 2006 How useful is SBF in predicting in vivo bone bioactivity? *Biomaterials* 27 2907–2915.

33. Mansur H S, Sadahira C M, Souza A N and Mansur A A P 2008 FTIR spectroscopy characterization of poly (vinyl alcohol) hydrogel with different hydrolysis degree and chemically crosslinked with glutaraldehyde *Mater. Sci. Eng. C* **28** 539-548

34. Ibarra J, Melendres J, Almada M, Burboa M G, Taboada P, Juárez J and Valdez M A 2015 Synthesis and characterization of magnetite/PLGA/chitosan nanoparticles *Mater. Res. Express* **2** 1-17

35. Wang S, Xue T, Niu B, Wei L and Wang H 2022 Preparation, characterization and antibacterial property of naringin loaded PLGA nanospheres *Prog. Nat. Sci.: Mater. Int.* **32** 498-503

36. Shurtakova D, Yavkin B, Gafurov M, Mamin G, Orlinskii S, Kuznetsova L, Bakhteev S, Ignatyev I, Smirnov I, Fedotov A, Komlev V 2019 Study of radiation-induced stable radicals in synthetic octacalcium phosphate by pulsed EPR Magn. Reson. Solids 21 19105.

37. Chen G, Zhang B and Zhao J 2015 Dispersion Process and Effect of Oleic Acid on Properties of Cellulose Sulfate-Oleic Acid Composite Film *Materials* ***8*** 2346-2360

38. Vologzhanina A V 2019 Intermolecular Interactions in Functional Crystalline Materials: From Data to Knowledge *Crystals* ***9*** 478

39. Tung M S, Tomazic B and Brown W E 1992 The effects of magnesium and fluoride on the hydrolysis of octacalcium phosphate *Arch. Oral Biol.* **37** 585-591

40. Gattazzo F, Urciuolo A, Bonaldo P, 2014 Extracellular matrix: A dynamic microenvironment for stem cell niche *Biochim. Biophys. Acta - Gen. Subj.* **1840** 2506-2519

41. Rongzhi Yang, Rui Wang, Saleheh Abbaspoor, Mariappan Rajan, Abduladheem Turki Jalil, Marwan Mahmood Saleh, Weizhuo Wang 2023 In vitro and in vivo evaluation of

hydrogel-based scaffold for bone tissue engineering application, *Arab. J. Chem* 16 (7) 104799.

42. Suzuki O, Kamakura S, Katagiri T, Nakamura M, Zhao B, Honda Y and Kamijo R 2006 Bone formation enhanced by implanted octacalcium phosphate involving conversion into Ca-deficient hydroxyapatite *Biomater.* **27** 2671-2681
43. Miyatake N, Kishimoto K N, Anada T, Imaizumi H, Itoi E and Suzuki O 2009 Effect of partial hydrolysis of octacalcium phosphate on its osteoconductive characteristics *Biomater.* **30** 1005-1014
44. Suzuki O, Yagishita H, Yamazaki M and Aoba T 1995 Adsorption of Bovine Serum Albumin onto Octacalcium Phosphate and its Hydrolyzates *Cells Mater.* **5** 45-54
45. Williams D F 2022 Biocompatibility pathways and mechanisms for bioactive materials: *The bioactivity zone Bioact. Mater.* **10** 306-322
46. Huzum B, Puha B, Necoara R M, Gheorghevici S, Puha G, Filip A, Sirbu P D and Alexa O 2021 Biocompatibility assessment of biomaterials used in orthopedic devices: An overview *Exp. Ther. Med.* **22** 1315
47. Uskoković V and Uskoković D P 2011 Nanosized hydroxyapatite and other calcium phosphates: chemistry of formation and application as drug and gene delivery agents *J. Biomed. Mater. Res. - Part B Appl. Biomater.* **96** 152-191
48. Zhou X, Zhang Z, Jiang W, Hu M, Meng Y, Li W, Zhou X and Wang C 2022 Naringenin is a Potential Anabolic Treatment for Bone Loss by Modulating Osteogenesis, Osteoclastogenesis, and Macrophage Polarization *Front. Pharmacol.* **13** 872188
49. Zhang L, He H, Zhang M, Wu Y, Xu X, Yang M and Mei L 2021 Assessing the Effect and Related Mechanism of Naringenin on the Proliferation, Osteogenic Differentiation and

Endothelial Differentiation of Human Periodontal Ligament Stem Cells *Biochem. Biophys. Res. Commun.* **534** 337-342

50. Kuiper J P, Puttlitz C M, Rawlinson J E, Dobbs R and Labus K M 2022 A mechanical evaluation of polyvinyl alcohol hydrogels for temporomandibular joint disc replacement *Front. Phy.* ***10*** 928579

51. E. R. Anishiya Chella Daisy, Mariappan Rajan, Kannan Suganya, Dhannia P. Narayanan, Jiang Zhu, Fungal keratitis infected eye treatment with antibiotic-loaded zinc ions tagged polyvinyl acetate phthalate-g-polypyrrole drug carrier, Journal of Saudi Chemical Society (2021) 25, 101347

52. Kim J, Kim S and Song I 2021 Biomimetic Octacalcium Phosphate Bone Has Superior Bone Regeneration Ability Compared to Xenogeneic or Synthetic Bone *Materials* **14** 5300

53. Noori S, Tavirani M R, Deravi N, Rabbani M I M and Zarghi A 2020 Naringenin Enhances the Anticancer Effect of Cyclophosphamide against MDA-MB-231 Breast Cancer Cells Via Targeting the STAT3 Signaling Pathway *Iran J. Pharm. Res.* **19** 122-133

54. Ito N, Kamitakahara M and Ioku K 2014 Preparation and evaluation of spherical porous granules of octacalcium phosphate/hydroxyapatite as drug carriers in bone cancer treatment *Mater. Lett.* **120** 94-96